The Quaternary Organization and Dynamics of the Molecular Chaperone HSP26 Are Thermally Regulated

Justin L.P. Benesch[1,10], **J. Andrew Aquilina**[2,10], **Andrew J. Baldwin**[3], **Agata Rekas**[4], **Florian Stengel**[1], **Robyn A. Lindner**[5], **Eman Basha**[6], **Glyn L. Devlin**[7], **Joseph Horwitz**[8], **Elizabeth Vierling**[6], **John A. Carver**[9,*], and **Carol V. Robinson**[1,*]

[1]Department of Chemistry, Physical and Theoretical Chemistry Laboratory, South Parks Road, Oxford OX1 3QZ, UK

[2]School of Biological Sciences, University of Wollongong, Wollongong, NSW 2522, Australia

[3]Departments of Molecular Genetics, Biochemistry, and Chemistry, University of Toronto, Toronto, ON, Canada

[4]National Deuteration Facility, Australian Nuclear Science and Technology Organisation, Lucas Heights, NSW 2234, Australia

[5]Tyrian Diagnostics, 35-41 Waterloo Road, North Ryde, NSW 2113, Australia

[6]Department of Chemistry & Biochemistry, University of Arizona, Tucson, AZ 85721, USA

[7]Department of Biochemistry & Molecular Biology, Monash University, Clayton, VIC 3800, Australia

[8]Jules Stein Eye Institute, University of California, Los Angeles, Los Angeles, CA 90095, USA

[9]School of Chemistry & Physics, The University of Adelaide, Adelaide, SA 5005, Australia

SUMMARY

The function of *Sc*HSP26 is thermally controlled: the heat shock that causes the destabilization of target proteins leads to its activation as a molecular chaperone. We investigate the structural and dynamical properties of *Sc*HSP26 oligomers through a combination of multiangle light scattering, fluorescence spectroscopy, NMR spectroscopy, and mass spec-trometry. We show that *Sc*HSP26 exists as a heterogeneous oligomeric ensemble at room temperature. At heat-shock temperatures, two shifts in equilibria are observed: toward dissociation and to larger oligomers. We examine the quaternary dynamics of these oligomers by investigating the rate of exchange of subunits between them and find that this not only increases with temperature but proceeds via two separate processes. This is consistent with a conformational change of the oligomers at elevated temperatures which regulates the disassembly rates of this thermally activated protein.

INTRODUCTION

The small heat-shock proteins (sHSPs) are an almost ubiquitous family of intracellular molecular chaperones, characterized by the presence of a highly conserved "α-crystallin" domain (Ecroyd and Carver, 2009; Haslbeck et al., 2005a; McHaourab et al., 2009; Narberhaus, 2002; van Montfort et al., 2001b). This domain is named after the eponymous

*Correspondence: john.carver@adelaide.edu.au (J.A.C.), carol.robinson@chem.ox.ac.uk (C.V.R.).
[10]These authors contributed equally to this work

vertebrate sHSP, which is found primarily in the eye lens (Kappé et al., 2003) and whose chaperone activity (Horwitz, 1992) is crucial to maintaining protein solubility (Brady et al., 1997). α-Crystallin is composed of two closely related subunits, A and B. In mammals, mutations to these proteins have been found to lead to cataract (Horwitz, 2003), and, with αB-crystallin being systemically expressed (Kappé et al., 2003), a number of devastating skeletal- and cardio-myopathies (Sun and MacRae, 2005).

The mechanism of action of the sHSPs is distinct from many molecular chaperones in that they do not actively refold target proteins. Instead, they bind partially unfolded targets and hold them in a state suitable for subsequent refolding by ATP-dependent chaperones (Ecroyd and Carver, 2009; Haslbeck et al., 2005a; McHaourab et al., 2009; Narberhaus, 2002; van Montfort et al., 2001b). This role of the sHSPs as the "paramedics" of the chaperone "medical service" is particularly apparent for *Sc*HSP26, one of two sHSPs in the *Saccharomyces cerevisiae* cytosol (Haslbeck et al., 2004). *Sc*HSP26 is activated rapidly by an increase in temperature (Franzmann et al., 2008) and stabilizes nonnative target proteins (Stromer et al., 2003) until the energy-dependent HSP104/Ssa1/Ydj1 refolding machinery is mobilized (Cashikar et al., 2005; Haslbeck, et al., 2005b). Consequently, these target proteins are recovered as folded functional entities (Cashikar et al., 2005; Haslbeck et al., 2005b).

Structurally, the sHSPs remain poorly understood because, in the main, members of this protein family are extremely dynamic and heterogenous (Haslbeck et al., 2005a; Horwitz, 2003). What is clear however is that, although the monomers are small, in general the sHSPs associate into large oligomers with dimeric units representing a common building block (Ecroyd and Carver, 2009; Haslbeck et al., 2005a; McHaourab et al., 2009; Narberhaus, 2002; van Montfort et al., 2001b). Presently, the highest resolution structural data for *Sc*HSP26 has been obtained by means of cryo-electron microscopy: though the proteins were heterogenous in structure, via the development of novel image processing strategies (White et al., 2004), two coexisting structures, each composed of 24 subunits, were obtained (White et al., 2006).

Here we examine *Sc*HSP26 principally by means of mass spectrometry (MS). With technological advances over the last decade enabling the transferral and analysis of intact protein complexes from solution into the gas phase (Benesch et al., 2007), MS has become a bona fide structural biology approach (Robinson et al., 2007). MS has been employed to determine the stoichiometries of a number of monodisperse sHSPs (Basha et al., 2010; Kennaway, et al., 2005), and to deconvolute the populations of individual oligomers within heterogeneous sHSP ensembles (Aquilina et al., 2003; Benesch et al., 2008; den Engelsman et al., 2009). Furthermore, real-time monitoring of the sHSPs has enabled us to describe and measure their dynamic quaternary structure through the process of subunit exchange (Painter et al., 2008; Sobott et al., 2002a).

Although this capacity of sHSPs to exchange subunits has been known for some time (van den Oetelaar et al., 1990), the cellular implications, including the role in chaperone action, remain unclear. It has been proposed that this phenomenon occurs to establish a dynamic and plastic chaperone ensemble, able to cater for the wide variety of target proteins destabilized under different stress conditions (Stengel et al., 2010). Additionally, the rate-determining dissociation of the oligomers (Bova et al., 2000) may amount to an activation of the sHSPs (van Montfort et al., 2001b; Haslbeck et al., 1999). However, it has since been shown for αA-crystallin that subunit exchange does not necessarily correlate with chaperone efficiency (Aquilina et al., 2005), and for *Sc*HSP26 that oligomer dissociation is not a prerequisite for activation (Franzmann et al., 2005). In the latter case, activation has been proposed to be controlled by temperature-induced changes in conformation of the "middle

domain," a region of sequence unique to ScHSP26 that is just N-terminal to the α-crystallin domain (Franzmann et al., 2008).

In the present work, we investigate the consequences of the transition to heat-shock temperatures on the quaternary structure and dynamics of ScHSP26. We demonstrate that, at room temperature, though the 24-mer stoichiometry is notably abundant, a range of oligomeric states are populated. At higher temperatures we notice a shift in equilibrium to favor monomers and dimers, but also that the predominant higher-order oligomeric species is a 40-mer. We examine the properties of these large oligomeric forms of ScHSP26 and show that not only are they dynamic, but also that the mechanism of their subunit exchange must involve more than one concurrent process.

RESULTS

ScHSP26 Populates a Polydisperse Ensemble That Exhibits Chaperone Activity

To investigate the mass distribution of the ScHSP26 oligomer at room temperature, we first used size-exclusion chromatography (SEC) coupled to a multiangle light-scattering (MALS) detector (Figure 1A). The protein eluted from the column as a single broad, but slightly asymmetric, peak centered on approximately 10.5 min. The MALS data shows that at the front end of the peak the average mass was approximately 950 kDa, at the tail end 580 kDa, and at the maximum 810 kDa. This corresponds to an approximate average-oligomer distribution range of 24–40 subunits.

The ability of ScHSP26 to act as a molecular chaperone was assessed via its inhibition of the aggregation and precipitation of reduced insulin B chain. Under reduction stress in this in vitro assay at 25°C, ScHSP26 was an efficient molecular chaperone, with a 1.0:1.0 ratio of ScHSP26:insulin providing complete suppression of aggregation (Figure 1B). The efficiency of chaperone action is comparable to that observed previously for ScHSP26 (Haslbeck et al., 1999) and in similar studies of other sHSPs (Nakamoto and Vigh, 2007).

ScHSP26 Undergoes Temperature- and Concentration-Dependent Structural Changes Leading to C-Terminal Exposure—The dependence of the structure of ScHSP26 on temperature was investigated by observing changes in intrinsic tryptophan fluorescence. There are two tryptophan residues in ScHSP26: Trp-72, which lies in the middle domain (Franzmann et al., 2008), and Trp-211, which resides in the C-terminal region (de Jong et al., 1998). Spectra acquired at 20°C, 45°C, and 90°C exhibit a substantial red shift with temperature (Figure 2A, left). Monitoring the intensity at 330 nm demonstrates a relatively uncooperative transition between 20°C and 45°C, with a midpoint of ~35°C (Figure 2A, right). Upon cooling of the solution back to 20°C, almost full recovery of a native-like spectrum could be observed within 12 hr. Together, these data indicate that the environment of one or both of the tryptophan residues in ScHSP26 becomes on average more solvent exposed with increasing temperature.

Sequence comparison suggests that the last few amino acids of ScHSP26, including Trp-211, are aligned with the C-terminal extension of the α-crystallins and other mammalian sHSPs (Figure 2B). This region is typically highly mobile and unstructured (Carver, 1999; Ghahghaei et al., 2009) and is downstream of the highly conserved C-terminal I/VXI/V motif, which serves to attach dimers together within sHSP structures (Haslbeck et al., 2005a; McHaourab et al., 2009; van Montfort et al., 2001b). Flexible regions in proteins can be observed in NMR experiments, despite belonging to species far beyond the accepted molecular mass limit of the technique, as they tumble essentially independently and hence more rapidly than the bulk oligomers (Carver et al., 1992). NMR spectra (^{1}H-^{1}H TOCSY and ^{1}H-^{15}N HSQC) were acquired at various temperatures and

protein concentrations in order to ascertain whether similar C-terminal flexibility is present in *Sc*HSP26 (Figure 2B). At 25°C and 1.66 mM, cross-peaks are observed only for Asn-213 (Figure 2BI). As the temperature was raised to 45°C a peak for Gly-212 was observed (Figure 2BII), and when the concentration was lowered to 0.33 mM at 45°C Trp-211 became visible (Fib 2BIII). At 0.17 mM and 45°C additional cross-peaks were observed at random-coil chemical shift values (Figure 2BIV). Thus, unlike the mammalian sHSPs (Carver et al., 1992), *Sc*HSP26 lacks a highly mobile C-terminal extension at 25°C. However, the appearance of additional cross peaks with elevated temperature and reduced concentration demonstrate enhanced C-terminal flexibility of *Sc*HSP26 under these conditions. Our data therefore combine to suggest that changes in intrinsic fluorescence with elevated temperature are due primarily to an alteration in structure which affects the solvent accessibility of Trp-211.

*Sc*HSP26 Undergoes Quaternary Rearrangement at Elevated Temperature

The temperature-dependent changes observed in our fluorescence and NMR data could feasibly arise from either changes in oligomerization or an unfolding of the protein chains. To address this, we examined *Sc*HSP26 organization at a range of temperatures by means of nanoelectrospray MS. Although our SEC-MALS data show that, at 25°C, under our conditions *Sc*HSP26 exists as a heterogeneous ensemble (Figure 1A), they only provide an average mass of the oligomers in the volume being sampled. In contrast, the high resolution afforded by MS renders it well suited to the analysis of complex protein assemblies (Sharon and Robinson, 2007). Figure 3A shows a mass spectrum of *Sc*HSP26 obtained at 25°C. A large number of peaks were observed between 9000 and 14,000 m/z in a bimodal distribution, with the first broad concentration of signal between approximately 9000 and 11,000 m/z, and the second between 11,000 and 14,000 m/z. The presence of this multitude of peaks suggests the presence of many differently sized oligomers and is in agreement with the SEC-MALS data. In the low m/z region of the spectrum, some minor peaks were observed corresponding to the presence of a small population of monomers and dimers.

To determine whether these monomers and dimers were in equilibrium with the oligomers, we obtained mass spectra at a range of different temperatures using a device that enables thermo-control of the sample solution during MS analysis (Benesch et al., 2003) (Figures 3B and 3C). As the temperature was raised, an increase in the amount of signal corresponding to monomer and dimer was observed. At 60°C, the highest temperature investigated, these dissociated species dominated the spectrum. The remaining intact oligomers were observed in the range of 11,000–14,000 m/z, corresponding to the higher m/z range of the two distributions observed at room temperature (Figure 3A). These results imply that a significant proportion of the monomers and dimers arose from dissociation of the smaller oligomers (i.e., those that appeared between 9000 and 11,000 m/z at room temperature, as the temperature was increased).

Polydisperse *Sc*HSP26 Is Composed of Dimeric Building Blocks and Has Variable Quaternary Organization

Because of the polydispersity of this system, the individual oligomeric species could not be completely identified. In the main, this is due to the poor level of desolvation afforded by the "gentle" MS conditions used in the heating experiments. In an attempt to improve desolvation, and consequently obtain narrower peak-widths and improved separation between peaks, the voltages accelerating the ions into the collision cell were increased. The resultant collisional activation leads to the removal of adducted buffer and solvent, and hence peaks of higher effective resolution (Benesch, 2009). Figure 4A shows such spectra of *Sc*HSP26 that had been equilibrated at 43°C for 30 min (lower panel) or had been left at room temperature (upper). The heat-treated protein displays peaks between 11,000 and

14,000 m/z. Two components, a 40-mer and 42-mer, could be clearly identified, although other minor peaks remained unassigned. In the unheated protein, peaks were distributed between 9000 and 14,000 m/z and were considerably more numerous than for the heat-treated sample. Although some species could be clearly identified, notably a 24-mer and 40-mer, the considerable peak overlap rendered further assignment problematic.

To facilitate the identification of all constituent species, we used a collision-induced dissociation approach that we have developed in our laboratory for the analysis of polydisperse assemblies (Aquilina et al., 2003). In such an experiment, the protein complexes are submitted to numerous high-energy collisions with an inert gas, which results in their dissociation into monomers and stripped oligomers (that is, oligomers having lost one or more monomers). The charge removed by the monomers is disproportionate to their mass, and thereby leads to a dramatic increase in the m/z ratio of the residual stripped oligomers. This dissociation process can occur repeatedly, in a sequential manner, leading to an effective charge reduction of the oligomers with a consequent increase in separation between peaks (Benesch et al., 2006; Benesch and Robinson, 2006). As such, the oligomeric distributions of the heterogeneous ensembles can be readily deconvoluted.

The results of this approach applied to the heat-treated *Sc*HSP26 are illustrated in Figure 4B. Activation of the oligomers gave rise to the appearance of four distributions of peaks: one centered on 2000 m/z corresponding to monomers, and others around 17,000 m/z, 24,000 m/z, and 35,000 m/z, corresponding to singly, doubly, and triply stripped oligomers, respectively. Figure 4C shows a portion of the spectrum from the doubly stripped oligomer region of the spectra for heat-treated (lower) and non-heat-treated (upper) *Sc*HSP26. The peak separation is such that the different oligomers comprising the heterogeneous ensemble can be identified. Nine distinct peaks were observed in the case of the nonheated protein, corresponding to oligomers containing even numbers of subunits in the range 24 to 40. For the heat-treated protein, the range was narrowed to 32 to 42.

Summing the intensities of the signal corresponding to the different species across the entire doubly stripped oligomer region allowed us to quantify the relative populations of the species that comprise the polydisperse assemblies (Figure 4D). The oligomeric distribution of unheated *Sc*HSP26 was found to have a range of 24 to 42 subunits, with no species containing an odd number of subunits. Notably, the distribution was non-Gaussian, with the 24-mer species being considerably more abundant than the "neighboring" 26-mer. After heat treatment, however, the distribution looked considerably different (Figure 4D, lower). No species smaller than 32 mers were observed, and the distribution was dominated by an oligomer composed of 40 subunits.

*Sc*HSP26 Exchanges Subunits by Different Pathways

In attempt to gain insight into the subunit dynamics of *Sc*HSP26, we used ^{15}N-labeled protein, which is 288 Da heavier per subunit than the wild-type (^{14}N) protein, yet of identical sequence and structure. Previously, we developed a technique of measuring the rate of subunit exchange for a mixture of two polydisperse proteins, in which the major overlapping peak of the doubly-stripped oligomer region for each protein is monitored (Aquilina et al., 2005). Because the major overlapping peak for a homo-oligomer in this region occurs at an m/z value equal to the mass of the monomer—that is, where all oligomers carry one charge per subunit (Aquilina et al., 2003)—it is possible to follow gross changes in the subunit composition of two heterogeneous ensembles over time.

An equimolar mixture of ^{14}N and [15]N *Sc*HSP26 was prepared and infused into a thermo-controlled nanospray probe set at 34°C (Figure 5A, upper panel). At the earliest time point, two distinct peaks were observed, one at ≈23,770 m/z and the other at ≈24090 m/z, which

correspond to the doubly stripped oligomers of all of the polydisperse assemblies of ^{14}N and [15]N ScHSP26, respectively. Over a period of 95 min, these peaks were observed to broaden and converge toward a midpoint at $\approx$23,940 m/z, consistent with a fully exchanged mixture of ScHSP26. This indicates exchange occurring in a stepwise manner, presumably via the incorporation of dimers. When this experiment was repeated at 39°C (Figure 5 middle panel), this convergence proceeded considerably more rapidly and was complete within 30 min. A third experiment performed at 45°C (Figure 5, bottom panel) showed a further increase in the exchange rate, such that the reaction mixture was equilibrated after approximately 12 min. In this case, the subunit exchange reaction characteristics were quite distinct from those observed at the lower temperature. Notably, during the reaction (e.g., after 5 min), the presence of both fully exchanged species as well as the original homogeneous isotope populations were observed.

To establish a more quantitative measure of the relative rates of exchange, we developed a model for the subunit exchange of ScHSP26 based on dimers dissociating from the oligomers with a rate constant of k_1^-, and associating with the next oligomer it encounters, such that the equilibrium distribution is maintained at all times. By simulating this subunit exchange process for a range of k_1^-, and comparing the outputs, we can determine the k_1^- value that best fits the data. Remarkably, but consistent with the qualitative change in subunit exchange profile we observe experimentally, we find it necessary to invoke a second rate constant, k_2^-, acting on a subpopulation of oligomers, to adequately fit the data at all temperatures (Figures 5B and 5C). This second rate constant is particularly large at 45°C, in accord with the notable "W-shaped" distribution of the heteroo-ligomers. From the temperature dependence of subunit exchange, we can extract activation energies of 97 ± 18 kJmol^{-1} and 483 ± 120 kJmol^{-1} for k_1^- and k_2^-, respectively (Figure 5D). This analysis shows that there is an increase in the rate of the overall reaction with temperature, however, with the temperature dependence of k_2^- being considerably more acute than for k_1^-. Although it is necessary to invoke two rate constants to explain the form of the data, it is not possible to unambiguously elucidate the nature of the second process. For example, two independent populations of oligomer, or different oliogmers having different dissociation rates, could reasonably explain the data. More complicated models involving additional free parameters could be constructed and will fit the data equally well, but cannot be statistically justified with the current data over this two-parameter model. The need to invoke a minimum of two rate constants in fitting the data clearly demonstrates that either at least two different modes of subunit exchange, or two types of oligomer with disparate exchange characteristics, exist.

DISCUSSION

Here we have reported on investigations into the oligomeric organization and dynamics of ScHSP26. Using both SEC-MALS and MS approaches, we have shown that at ambient temperature this protein exists as a polydisperse ensemble comprising numerous oligomeric states. Previous reports have suggested the presence of multiple oligomeric states for ScHSP26 (Bentley et al., 1992; Ferreira et al., 2006), but here we have quantified their relative populations. Using a tandem MS technique, we have demonstrated the 24-mer to be "anomalously" abundant at 25°C, consistent with previous reports that have culminated in a cryo-electron microscopy-derived 3D structure of this oligomeric state (White et al., 2006). However, we show here that ScHSP26 also forms larger oligomers, up to 42 subunits in size at room temperature. The oligomers observed were composed exclusively of an even number of subunits. This strongly suggests there to be a basic dimeric "building block," an observation consistent with the cryo-electron microscopy reconstruction of the ScHSP26 24-mer (White et al., 2006), as well as structural studies of other sHSPs (Haslbeck et al., 2005a; Narberhaus, 2002; van Montfort et al., 2001b).

The activity of *Sc*HSP26 is known to be temperature dependent, such that it only exhibits optimal chaperone function at heat shock temperatures (Haslbeck et al., 1999). Here, we investigated the effect of temperature on the oligomeric structure of *Sc*HSP26 by using a combined approach of tryptophan fluorescence, NMR, and thermo-controlled MS. We found that an increase in temperature leads to the equilibrium shifting to monomers and dimers with partially flexible C-terminal extensions, such that at the highest temperature measured these suboligomeric species dominated the spectrum. Although these data show that the individual subunits undergo partial unfolding at higher temperature, they also indicate that, unlike in mammalian sHSPs (Carver et al., 1992; Carver and Lindner, 1998), this region is not unstructured and highly mobile at 25°C. This agrees with the fact that a hydrophobic tryptophan is the pen-penultimate residue in *Sc*HSP26 which, at ambient temperature, would be energetically costly to be located in a flexible and fully solvent-exposed region of the protein. Indeed, our previous studies showed that inserting a tryptophan residue into the C-terminal extension of the sHSP αA-crystallin led to a reduction in flexibility of the extension (Smulders et al., 1996). As such, it appears that a long and flexible C-terminal extension is a property of the polydisperse mammalian sHSPs.

Redistribution of oligomers into monomers and dimers at elevated temperature and in dilute solution has previously been observed for *Sc*HSP26 (Haslbeck et al., 1999) and other sHSPs (Benesch et al., 2003; Giese and Vierling, 2002; van Montfort et al., 2001a). Examination of the oligomeric region of the mass spectrum at elevated temperature revealed the remaining *Sc*HSP26 to exist in forms of 32 subunits or larger, with the majority existing as a 40-mer. These large oligomers therefore are thermodynamically favored at higher temperatures and represent the oligomeric forms that are present under conditions during which *Sc*HSP26 is active as a chaperone. Such an increase in oligomeric size at elevated temperatures has also been observed for the dodecameric sHSPs HSP16.9 from wheat (Benesch et al., 2003), HSP18.1 from pea (Stengel et al., 2010), and the polydisperse αB-crystallin (Sun and Liang, 1998). This increase in size may therefore represent a mechanism of activation for the sHSPs.

To probe the inherent dynamics of this previously unreported range of oligomeric states that form at higher temperatures, we monitored their subunit exchange in real time by means of MS. We found that *Sc*HSP26 exchanged subunits in a stepwise manner such that at 34°C complete equilibration occurred after approximately 95 min. At 39°C, this reaction was complete in about 30 min, which is very similar to the time scale for the exchange of the A and B subunits of α-crystallin at this temperature (Aquilina et al., 2005). However, increasing the temperature to 45°C resulted in the exchange reaction apparently occurring via a different regime such that at intermediate reaction times populations of both unexchanged and fully exchanged oligomers were present. Detailed comparison with the data and in silico modeling of subunit exchange revealed that two parameters are required to adequately describe subunit exchange of *Sc*HSP26 at all temperatures investigated here. The need for a two-parameter fit may reflect the existence of multiple conformations of the same oligomers, potentially with differing activity or chaperoning roles.

An elegant fluorescence study has shown that the conformation of the middle domain of *Sc*HSP26 undergoes rearrangement as the temperature is increased, resulting in chaperone-active oligomers (Franzmann et al., 2008). Furthermore, this was shown to be a biphasic process. Taking our results in the context of these observations provides a possibility that the different middle-domain-conformers of *Sc*HSP26 exchange subunits at different rates, with the active form being more dynamic. Two distinct conformers of the *Sc*HSP26 24-mer have been revealed by cryo-electron microscopy (White et al., 2006) and also for the related *Archaeoglobus fulgidus* HSP20.2 and *Methanocaldococcus jannaschii* HSP16.5 (Haslbeck et al., 2008). A temperature-dependent shift in the relative populations of these

conformations was observed in the archaeal proteins (Haslbeck et al. 2008), suggesting that they may reflect forms of differing activity. Considering all these observations together, a complex picture of the mechanism of thermal activation of *Sc*HSP26 emerges. At low temperatures, the heterogeneous ensemble of *Sc*HSP26 is dynamic, with subunits exchanging freely between oligomers. The rate of this exchange becomes more rapid as the temperature is increased, with the oligomers that comprise the ensemble being, on average, larger than those at low temperatures. Concomitant to this, the middle domain undergoes a conformational change that leads to a highly dynamic oligomeric form with high chaperone activity.

The role of subunit exchange, via the dissociation and reassociation of subunits, in sHSP chaperone action in vivo is not well understood. It appears, for *Sc*HSP26 at least, that complete dissociation of dimers from the oligomers is not a prerequisite for chaperone activity (Franzmann et al., 2005). However dissociation is effectively a continuous process, and it may be that surfaces required for binding become exposed as a result of structural relaxation during the dissociation process. Although only two sHSPs are present in S*accharomyces cerevisiae* (Haslbeck et al., 2004), it is clear that the genome of many species encode numerous sHSPs (Haslbeck et al., 2005a) and that those members of the same evolutionary class found in the same cellular compartment will form a range of heterocomplexes in vivo (Painter et al., 2008). If the oligomers themselves are the active chaperones, then this would provide a large array of species, potentially all with different target protein affinities and specificities (Stengel et al., 2010). As such, the primary function of subunit exchange of the sHSPs could be to establish and maintain this chaperone ensemble, thereby providing broad stress and target protein specificity.

SIGNIFICANCE

Through the detailed interrogation of *Sc*HSP26, this study highlights how fluctuations in both the quaternary structure and dynamics of proteins govern their function (Henzler-Wildman and Kern, 2007; Smock and Gierasch, 2009). Elucidating the details of these properties however is hampered by the heterogeneous nature of many protein assemblies. As we have demonstrated here, this can be overcome by exploiting the high resolution of separation afforded by MS. Integrating MS measurements, which report on the properties of individual oligomers, with those derived from biophysical methods which report on the level of the constituent monomers (such as fluorescence and NMR spectros-copies here) therefore provides an attractive and general "hybrid" approach for the study of proteins that populate heterogeneous oligomeric ensembles.

EXPERIMENTAL PROCEDURES

Protein Preparation

*Sc*HSP26 was expressed in *Escherichia coli* BL21 strain using standard methods. For uniformly ^{15}N-labeled protein, cells were grown in minimal medium containing ^{15}N-labeled ammonium chloride with 200 μg/ml carbenicillin at 32°C. *Sc*HSP26 purification from the soluble cell fraction was performed as described elsewhere (Basha et al., 2004), with the following modifications. Protein was enriched in the 60%–90% (w/v) ammonium sulfate fraction, and elution of the protein from the DEAE column (diethylaminoethyl-Sepharose Fast Flow resin; Sigma) was performed using a 0–400 mM sodium chloride gradient.

Size-Exclusion Chromatography and Light Scattering

*Sc*HSP26 was analyzed by using size-exclusion chromatography with on-line light scattering, absorbance, and refractive index detectors (Wen et al., 1996). A Bio-Sil 400 column (Bio-Rad) was connected in-line to a UV detector (Amersham Biosciences

UV-900), a DAWN-EOS (Wyatt Technology) laser light scattering detector, and an Optilab-DSP (Wyatt Technology) refractive index detector. Samples were loaded onto the column at a concentration of 1.5 mg/ml and eluted with 50 mM phosphate buffer (pH 7.2) containing 100 mM sodium chloride (PBS).

Chaperone Assay

Bovine pancreatic insulin (0.25 mg/ml) was incubated at 25°C for 100 min in PBS (pH 7.2). Aggregation and precipitation were initiated by addition of DTT to a final concentration of 10 mM. *Sc*HSP26 was added from a 5 mg/ml stock to give the final w/w ratios indicated.

Fluorescence Spectroscopy

*Sc*HSP26 was diluted to 0.025 mg/ml in 100 mM ammonium acetate at pH 7.3 and heated from 20–90°C at 1°C/min on a Carey Eclipse fluorescence spectrophotometer. The sample was excited at 280 nm, and emission was recorded at 330 nm. Fluorescence spectra were also recorded at three temperatures to provide more information on the structural transitions.

NMR Spectroscopy

^1H and ^{15}N NMR spectra were acquired at magnetic field strength corresponding to a ^1H resonance frequency of 500 MHz on a Varian Inova-500 spectrometer equipped with a triple-resonance pulsed-field gradient probe; 1.66, 0.33, or 0.17 mM ^{15}N-labeled *Sc*HSP26 was dissolved in 20 mM sodium phosphate buffer (pH 6.5), containing 10% D_2O, 0.02% NaN_3. ^1H-^{15}N 2D HSQC spectra (Kay et al., 1992) were acquired at 25°C and 45°C with 16 transients per increment in the direct dimension (^1H) and 256 increments in the ^{15}N dimension. Spectral widths were 6000 Hz in the ^1H dimension and 1000 Hz in the ^{15}N dimension. ^1H-^1H Watergate TOCSY spectra (Piotto et al., 1992) with ^{15}N-decoupling were acquired at various temperatures between 20 and 60°C over a spectral width of 6000 Hz in both dimensions, with 256 t_1 increments, 80 transients per increment using spin-lock periods of 30 and 50 ms. All NMR spectra were processed using Varian VNMR software (version 6.1c).

Nanoelectrospray Mass Spectrometry

Samples of ^{14}N and ^{15}N-labeled *Sc*HSP26 were prepared for MS analysis by loading them onto a Superdex 200HR10/30 gel filtration column (GE Healthcare) and eluting at 0.3 ml/min with 200 mM ammonium acetate at 6°C. The resulting fractions corresponding to the protein oligomers were combined and concentrated with a centrifugal filtration device (Millipore Biomax), to give final protein concentrations of 1.3 mg/ml.

MS experiments were conducted using a previously described protocol (Hernández and Robinson, 2007) on a Q-ToF 2 mass spectrometer (Waters) that had been modified for high-mass operation (Sobott et al., 2002b). Conditions were carefully chosen to allow the ionization and detection of the proteins without disrupting the noncovalent interactions that maintain the quaternary structure. The following instrument voltages and pressures were used: capillary 1.7 kV, sample cone 100 V, collision cell voltage 10 V, ion transfer stage pressure 9.0×10^{-3} mbar, quadrupole analyzer pressure 9.5×10^{-4} mbar, ToF analyzer pressure 1.7×10^{-6} mbar, and 10 μbar of argon in the collision cell. Sample heating was performed using an online thermo-controlled nano-ESI device designed in-house (Benesch et al., 2003). To effect dissociation, gas-phase oligomers were collided with argon atoms in the collision cell of the mass spectrometer. This was achieved by increasing the accelerating voltage into the collision cell and raising the gas pressure within to 35 μbar. Values in the range of 20–200 V were used for this parameter, depending on the extent of dissociation desired. The lower values were used to remove adducted solvent and buffer, thereby

reducing peak width, and the higher values were used to effect actual dissociation of the oligomers (Benesch, 2009). Relative protein abundances were extracted by comparing peak intensities across the doubly stripped oligomer region (Aquilina et al., 2003).

Subunit Exchange

Subunit exchange analyses were performed at 34°C, 39°C, and 45°C using the thermo-controlled nanoelectrospray probe. Equal volumes of the ^{14}N and ^{15}N-labeled ScHSP26 were mixed immediately prior to analysis, and acquisition of spectra was initiated within a 60 s equilibration period. To quantify our data, we fitted the experimental data to a model for subunit exchange, described as follows.

The oligomerization of sHSPs can be modeled as a series of consecutive equilibria of the form $P_{i-1}+P_1 \rightleftharpoons P_i$, where P_i denotes an oligomer of size i, as described previously (Stengel, et al., 2010). For each step, a stepwise association constant can be defined as $K_i = [P_i]/[P_{i-1}][P_1] = k_i^+/k_i^-$, with a corresponding free energy $\Delta G_i = RT \ln [P_i]/[P_{i-1}][P_1]$. The rate of change of each oligomer will then be given by:

$$\frac{d[P_i]}{dt} = -ik_i^-[P_i] + k_i^+[P_{i-1}][P_1] + (i+1)k_{i+1}^-[P_{i+1}] - k_{i+1}^+[P_i][P_1],$$

where the dissociation of each individual subunit within an oligomer is assumed to be equally probable. From a series of experimentally determined oligomer populations together with the concentration of free subunits at a given condition it is possible, therefore, to determine the ratio k_i^+/k_i^-. In the subunit exchange experiments here, ^{14}N and ^{15}N-labeled ScHSP26 is mixed. In such a situation, the rate of change of a given oligomer comprising i 'light' and j 'heavy' subunits will be given by:

$$\frac{d[P_{i,j}]}{dt} = \begin{aligned}[t] & -(i+j)k_{i+j}^-[P_{i,j}] + k_{i+j}^+([P_{1,0}][P_{i,j-1}] + [P_{0,1}][P_{i-1,j}]) \\ & + (i+j+1)k_{i+j+1}^-([P_{i,j+1}] + [P_{i+1,j}]) - k_{i+j+1}^+([P_{1,0}] + [P_{0,1}])[P_{i,j}]. \end{aligned}$$

Starting from the initial condition that oligomers of the form $[P_{i,0}]$ and $[P_{0,j}]$ have their equilibrium values, we can simulate the subunit exchange process that ultimately leads to heterogeneous oligomers with $i = j$ being the most populated for any set of oligomers of size $i+j$. The simplest method to fit the model to the kinetic data is to fit the data to one rate constant. We can accomplish this by assuming the dissociation rate for a monomer to leave an oligomer is independent of oligomer size ($k_i^- - k^-$). By following the variation of this constant as a function of temperature, we can estimate the activation parameters of the subunit exchange process.

Although the 30°C and 39°C data fit well to this model, the 45°C data do not, suggesting that the subunit exchange process is more complex. There are several ways in which this extra complexity can be introduced. The 45°C data can be explained by specifying that a minor proportion of the oligomers have a significantly faster dissociation rate than the bulk. Thus, the kinetic data have to be fitted globally to three constants: a "fast" dissociation constant, a "slow" dissociation constant, and the proportion of fast/slow oligomers. The relative proportion of the two oligomer types is mainly specified by the 45°C data equating to ~25% of the total oligomers. Using the value obtained from fitting these data when fitting the 30°C and 39°C data gives a significantly reduced χ^2 relative to the one parameter fits.

Acknowledgments

REFERENCES

Aquilina JA, Benesch JLP, Bateman OA, Slingsby C, Robinson CV. Polydispersity of a mammalian chaperone: mass spectrometry reveals the population of oligomers in alphaB-crystallin. Proc. Natl. Acad. Sci. USA. 2003; 100:10611–10616. [PubMed: 12947045]

Aquilina JA, Benesch JLP, Ding LL, Yaron O, Horwitz J, Robinson CV. Subunit exchange of polydisperse proteins: mass spectrometry reveals consequences of alphaA-crystallin truncation. J. Biol. Chem. 2005; 280:14485–14491. [PubMed: 15701626]

Basha E, Jones C, Wysocki V, Vierling E. Mechanistic differences between two conserved classes of small heat shock proteins found in the plant cytosol. J. Biol. Chem. 2010; 285:11489–11497. [PubMed: 20145254]

Basha E, Lee GJ, Demeler B, Vierling E. Chaperone activity of cytosolic small heat shock proteins from wheat. Eur. J. Biochem. 2004; 271:1426–1436. [PubMed: 15066169]

Benesch JLP. Collisional activation of protein complexes: picking up the pieces. J. Am. Soc. Mass Spectrom. 2009; 20:341–348. [PubMed: 19110440]

Benesch JLP, Robinson CV. Mass spectrometry of macromolecular assemblies: preservation and dissociation. Curr. Opin. Struct. Biol. 2006; 16:245–251. [PubMed: 16563743]

Benesch JLP, Sobott F, Robinson CV. Thermal dissociation of multimeric protein complexes by using nanoelectrospray mass spectrometry. Anal. Chem. 2003; 75:2208–2214. [PubMed: 12918957]

Benesch JLP, Aquilina JA, Ruotolo BT, Sobott F, Robinson CV. Tandem mass spectrometry reveals the quaternary organization of macromolecular assemblies. Chem. Biol. 2006; 13:597–605. [PubMed: 16793517]

Benesch JLP, Ruotolo BT, Simmons DA, Robinson CV. Protein complexes in the gas phase: technology for structural genomics and proteomics. Chem. Rev. 2007; 107:3544–3567. [PubMed: 17649985]

Benesch JLP, Ayoub M, Robinson CV, Aquilina JA. Small heat shock protein activity is regulated by variable oligomeric substructure. J. Biol. Chem. 2008; 283:28513–28517. [PubMed: 18713743]

Bentley NJ, Fitch IT, Tuite MF. The small heat-shock protein Hsp26 of *Saccharomyces cerevisiae* assembles into a high molecular weight aggregate. Yeast. 1992; 8:95–106. [PubMed: 1561840]

Bova MP, McHaourab HS, Han Y, Fung BK. Subunit exchange of small heat shock proteins: analysis of oligomer formation of alphaA-crystallin and Hsp27 by fluorescence resonance energy transfer and site-directed truncations. J. Biol. Chem. 2000; 275:1035–1042. [PubMed: 10625643]

Brady JP, Garland D, Duglas-Tabor Y, Robison WG Jr. Groome A, Wawrousek EF. Targeted disruption of the mouse alpha A-crystallin gene induces cataract and cytoplasmic inclusion bodies containing the small heat shock protein alphaB-crystallin. Proc. Natl. Acad. Sci. USA. 1997; 94:884–889. [PubMed: 9023351]

Carver JA. Probing the structure and interactions of crystallin proteins by NMR spectroscopy. Prog. Retin. Eye Res. 1999; 18:431–462. [PubMed: 10217479]

Carver JA, Lindner RA. NMR spectroscopy of alpha-crystallin: insights into the structure, interactions and chaperone action of small heat-shock proteins. Int. J. Biol. Macromol. 1998; 22:197–209. [PubMed: 9650074]

Carver JA, Aquilina JA, Truscott RJ, Ralston GB. Identification by 1H NMR spectroscopy of flexible C-terminal extensions in bovine lens alpha-crystallin. FEBS Lett. 1992; 311:143–149. [PubMed: 1397302]

Cashikar AG, Duennwald M, Lindquist SL. A chaperone pathway in protein disaggregation. Hsp26 alters the nature of protein aggregates to facilitate reactivation by Hsp104. J. Biol. Chem. 2005; 280:23869–23875. [PubMed: 15845535]

de Jong WW, Caspers GJ, Leunissen JA. Genealogy of the alpha-crystallin—small heat-shock protein superfamily. Int. J. Biol. Macromol. 1998; 22:151–162. [PubMed: 9650070]

den Engelsman J, Boros S, Dankers PY, Kamps B, Vree Egberts WT, Bode CS, Lane LA, Aquilina JA, Benesch JLP, Robinson CV, et al. The small heat-shock proteins HSPB2 and HSPB3 form well-defined heterooligomers in a unique 3 to 1 subunit ratio. J. Mol. Biol. 2009; 393:1022–1032. [PubMed: 19715703]

Ecroyd H, Carver JA. Crystallin proteins and amyloid fibrils. Cell. Mol. Life Sci. 2009; 66:62–81. [PubMed: 18810322]

Ferreira RM, de Andrade LR, Dutra MB, de Souza MF, Flosi Paschoalin VM, Silva JT. Purification and characterization of the chaperone-like Hsp26 from *Saccharomyces cerevisiae*. Protein Expr. Purif. 2006; 47:384–392. [PubMed: 16603379]

Franzmann TM, Wuhr M, Richter K, Walter S, Buchner J. The activation mechanism of Hsp26 does not require dissociation of the oligomer. J. Mol. Biol. 2005; 350:1083–1093. [PubMed: 15967461]

Franzmann TM, Menhorn P, Walter S, Buchner J. Activation of the chaperone Hsp26 is controlled by the rearrangement of its thermosensor domain. Mol. Cell. 2008; 29:207–216. [PubMed: 18243115]

Ghahghaei A, Rekas A, Carver JA, Augusteyn RC. Structure/function studies of dogfish alpha-crystallin, comparison with bovine alpha-crystallin. Mol. Vis. 2009; 15:2411–2420. [PubMed: 19956560]

Giese KC, Vierling E. Changes in oligomerization are essential for the chaperone activity of a small heat shock protein in vivo and in vitro. J. Biol. Chem. 2002; 277:46310–46318. [PubMed: 12297515]

Haslbeck M, Walke S, Stromer T, Ehrnsperger M, White HE, Chen S, Saibil HR, Buchner J. Hsp26: a temperature-regulated chaperone. EMBO J. 1999; 18:6744–6751. [PubMed: 10581247]

Haslbeck M, Braun N, Stromer T, Richter B, Model N, Weinkauf S, Buchner J. Hsp42 is the general small heat shock protein in the cytosol of *Saccharomyces cerevisiae*. EMBO J. 2004; 23:638–649. [PubMed: 14749732]

Haslbeck M, Franzmann T, Weinfurtner D, Buchner J. Some like it hot: the structure and function of small heat-shock proteins. Nat. Struct. Mol. Biol. 2005a; 12:842–846.

Haslbeck M, Miess A, Stromer T, Walter S, Buchner J. Disassembling protein aggregates in the yeast cytosol. The cooperation of Hsp26 with Ssa1 and Hsp104. J. Biol. Chem. 2005b; 280:23861–23868. [PubMed: 15843375]

Haslbeck M, Kastenmuller A, Buchner J, Weinkauf S, Braun N. Structural dynamics of archaeal small heat shock proteins. J. Mol. Biol. 2008; 378:362–374. [PubMed: 18353362]

Henzler-Wildman K, Kern D. Dynamic personalities of proteins. Nature. 2007; 450:964–972. [PubMed: 18075575]

Hernández H, Robinson CV. Determining the stoichiometry and interactions of macromolecular assemblies from mass spectrometry. Nat. Protoc. 2007; 2:715–726. [PubMed: 17406634]

Horwitz J. Alpha-crystallin can function as a molecular chaperone. Proc. Natl. Acad. Sci. USA. 1992; 89:10449–10453. [PubMed: 1438232]

Horwitz J. Alpha-crystallin. Exp. Eye Res. 2003; 76:145–153. [PubMed: 12565801]

Kappé G, Franck E, Verschuure P, Boelens WC, Leunissen JA, de Jong WW. The human genome encodes 10 alpha-crystallin-related small heat shock proteins: HspB1-10. Cell Stress Chaperones. 2003; 8:53–61. [PubMed: 12820654]

Kay LE, Keifer P, Saarinen T. Pure absorption gradient enhanced heteronuclear single quantum correlation spectroscopy with improved sensitivity. J. Am. Chem. Soc. 1992; 114:10663–10665.

Kennaway CK, Benesch JLP, Gohlke U, Wang L, Robinson CV, Orlova EV, Saibil HR, Keep NH. Dodecameric structure of the small heat shock protein Acr1 from *Mycobacterium tuberculosis*. J. Biol. Chem. 2005; 280:33419–33425. [PubMed: 16046399]

McHaourab HS, Godar JA, Stewart PL. Structure and mechanism of protein stability sensors: chaperone activity of small heat shock proteins. Biochemistry. 2009; 48:3828–3837. [PubMed: 19323523]

Nakamoto H, Vigh L. The small heat shock proteins and their clients. Cell. Mol. Life Sci. 2007; 64:294–306. [PubMed: 17187175]

Narberhaus F. Alpha-crystallin-type heat shock proteins: socializing minichaperones in the context of a multichaperone network. Microbiol. Mol. Biol. Rev. 2002; 66:64–93. [PubMed: 11875128]

Painter AJ, Jaya N, Basha E, Vierling E, Robinson CV, Benesch JLP. Real-time monitoring of protein complexes reveals their quaternary organization and dynamics. Chem. Biol. 2008; 15:246–253. [PubMed: 18355724]

Piotto M, Saudek V, Sklenar V. Gradient-tailored excitation for single-quantum NMR spectroscopy of aqueous solutions. J. Biomol. NMR. 1992; 2:661–665. [PubMed: 1490109]

Robinson CV, Sali A, Baumeister W. The molecular sociology of the cell. Nature. 2007; 450:973–982. [PubMed: 18075576]

Sharon M, Robinson CV. The role of mass spectrometry in structure elucidation of dynamic protein complexes. Annu. Rev. Biochem. 2007; 76:167–193. [PubMed: 17328674]

Smock RG, Gierasch LM. Sending signals dynamically. Science. 2009; 324:198–203. [PubMed: 19359576]

Smulders RHPH, Carver JA, Lindner RA, van Boekel MA, Bloemendal H, de Jong WW. Immobilization of the C-terminal extension of bovine alphaA-crystallin reduces chaperone-like activity. J. Biol. Chem. 1996; 271:29060–29066. [PubMed: 8910559]

Sobott F, Benesch JLP, Vierling E, Robinson CV. Subunit exchange of multimeric protein complexes: real-time monitoring of subunit exchange between small heat shock proteins by using electrospray mass spectrometry. J. Biol. Chem. 2002a; 277:38921–38929. [PubMed: 12138169]

Sobott F, Hernández H, McCammon MG, Tito MA, Robinson CV. A tandem mass spectrometer for improved transmission and analysis of large macromolecular assemblies. Anal. Chem. 2002b; 74:1402–1407. [PubMed: 11922310]

Stengel F, Baldwin AJ, Painter AJ, Jaya N, Basha E, Kay LE, Vierling E, Robinson CV, Benesch JLP. Quaternary dynamics and plasticity underlie small heat shock protein chaperone function. Proc. Natl. Acad. Sci. USA. 2010; 107:2007–2012. [PubMed: 20133845]

Stromer T, Ehrnsperger M, Gaestel M, Buchner J. Analysis of the interaction of small heat shock proteins with unfolding proteins. J. Biol. Chem. 2003; 278:18015–18021. [PubMed: 12637495]

Sun TX, Liang JJ. Intermolecular exchange and stabilization of recombinant human alphaA- and alphaB-crystallin. J. Biol. Chem. 1998; 273:286–290. [PubMed: 9417077]

Sun Y, MacRae TH. The small heat shock proteins and their role in human disease. FEBS J. 2005; 272:2613–2627. [PubMed: 15943797]

van den Oetelaar PJ, van Someren PF, Thomson JA, Siezen RJ, Hoenders HJ. A dynamic quaternary structure of bovine alpha-crystallin as indicated from intermolecular exchange of subunits. Biochemistry. 1990; 29:3488–3493. [PubMed: 2354148]

van Montfort RL, Basha E, Friedrich KL, Slingsby C, Vierling E. Crystal structure and assembly of a eukaryotic small heat shock protein. Nat. Struct. Biol. 2001a; 8:1025–1030. [PubMed: 11702068]

van Montfort R, Slingsby C, Vierling E. Structure and function of the small heat shock protein/alpha-crystallin family of molecular chaperones. Adv. Protein Chem. 2001b; 59:105–156. [PubMed: 11868270]

Wen J, Arakawa T, Philo JS. Size-exclusion chromatography with on-line light-scattering, absorbance, and refractive index detectors for studying proteins and their interactions. Anal. Biochem. 1996; 240:155–166. [PubMed: 8811899]

White HE, Saibil HR, Ignatiou A, Orlova EV. Recognition and separation of single particles with size variation by statistical analysis of their images. J. Mol. Biol. 2004; 336:453–460. [PubMed: 14757057]

White HE, Orlova EV, Chen S, Wang L, Ignatiou A, Gowen B, Stromer T, Franzmann TM, Haslbeck M, Buchner J, Saibil HR. Multiple distinct assemblies reveal conformational flexibility in the small heat shock protein Hsp26. Structure. 2006; 14:1197–1204. [PubMed: 16843901]
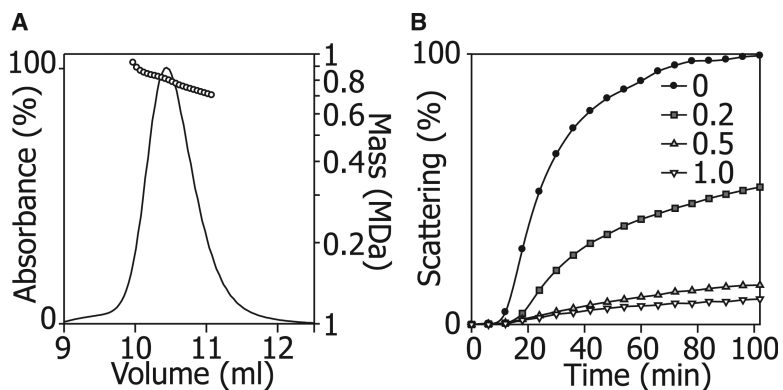
Figure 1. Oligomeric Distribution and Chaperone Activity of *Sc*HSP26

(A) *Sc*HSP26 examined by SEC-MALS illustrates the heterogeneity of the oligomeric ensemble. The molecular mass decreased across the peak from 950 kDa to 580 kDa and was centered around a maximum population species of 810 kDa, corresponding to an approximately 34 subunit oligomer.

(B) Insulin reduction assay of the chaperone action of *Sc*HSP26. At 25°C, in the absence of *Sc*HSP26, insulin B chain is reduced and exhibits an apparent increase in absorbance at 360 nm due to light scattering over a period of 100 min as a result of aggregation. At a subunit molar ratio of 0.2:1.0 *Sc*HSP26:insulin, a 50% reduction in aggregation was observed due to the chaperone action of *Sc*HSP26. At the higher ratios of 0.5:1.0 and 1.0:1.0, almost complete suppression of aggregation is achieved.
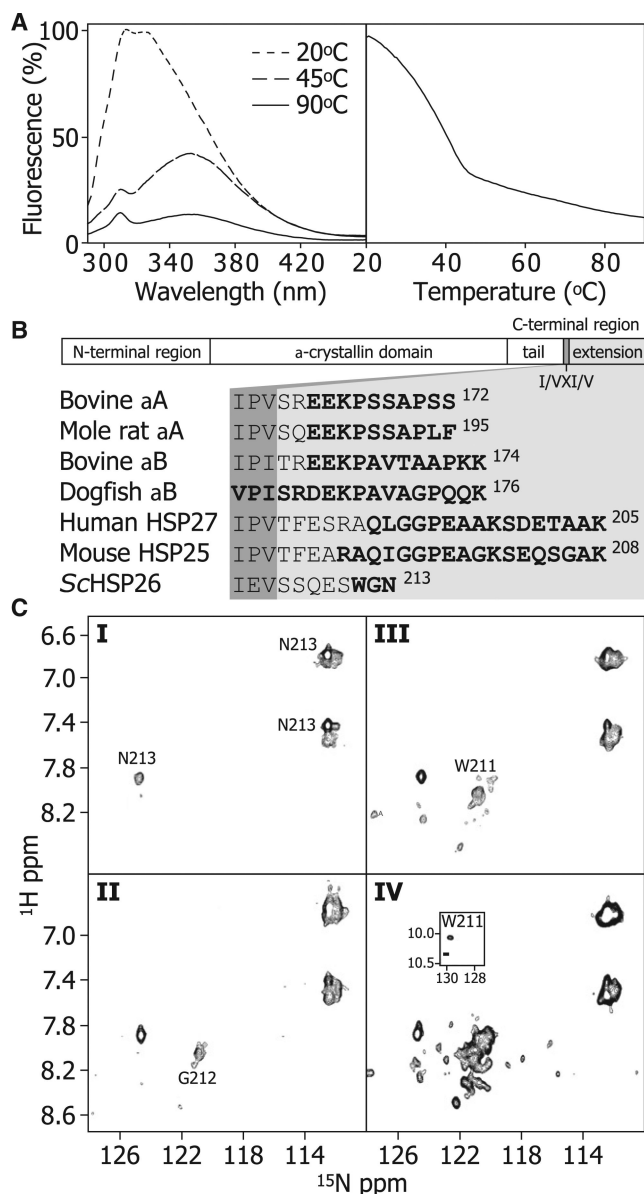
Figure 2. C-Terminal Flexibility of *Sc*HSP26

(A) The dependence of tertiary/quaternary structure of the *Sc*HSP26 oligomers on temperature was examined by observing the changes in intrinsic tryptophan fluorescence. *Sc*HSP26 was heated from 20–90°C at 1°C/min (right). The sample was excited at 280 nm and emission was recorded at 330 nm. The resultant melt demonstrated that the tryptophan residues became significantly more solvent exposed between 20°C and 45°C, whereas a much smaller, linear decrease in fluorescence was observed up to 90°C. Fluorescence spectra were also recorded at three temperatures to provide information on the structural transitions (left). At 20°C, the emission spectrum has a λ_{max} at ≈325 nm. At 45°C, there was a decrease in the emission intensity concomitant with a dramatic shift in the λ_{max} to 352 nm. At 90°C, a further decrease in fluorescence intensity but no λ_{max} shift occurred. These data indicate that the majority of the tertiary structure in the vicinity of the tryptophan residues is lost during the initial unfolding transition.

(B) The primary sequence of sHSPs in general is composed of an N-terminal region, the α-crystallin domain, and a C-terminal region. The latter is subdivided into a C-terminal tail,

and a C-terminal extension, separated by the conserved I/VXI/V motif. The sequence of *Sc*HSP26 is aligned to those of animal sHSPs which have been demonstrated to contain flexible C-terminal extensions. Residues which are clearly identified by NMR spectroscopy measurements are highlighted in bold.

(C) ^{1}H-^{15}N 2D HSQC NMR spectra of *Sc*HSP26 at I: 25°C and 1.66 mM; II: 45°C and 1.66 mM; III: 45°C and 0.33 mM; IV: 45°C and 0.17 mM. At the same concentration (1.66 mM), solutions of HSP26 exhibit a minor enhancement of C-terminal flexibility with increased temperature, as evidenced by the greater number of cross-peaks resolved at random coil chemical shift values and an additional cross-peak from G212 (I and II). At 45°C, 5- and 10-fold dilution an increased number of cross-peaks are observed (III and IV), suggesting greater C-terminal flexibility. This is consistent with an overall loosening of the structure and smaller, less-structured species of *Sc*HSP26 being present under more dilute conditions.
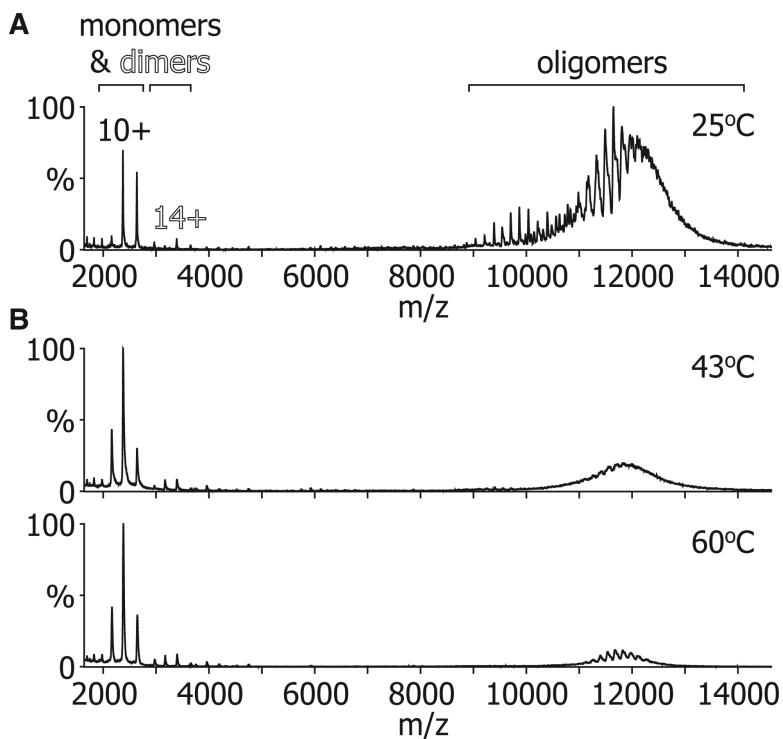
Figure 3. MS Demonstrates a Temperature-Dependent Dissociation of *Sc*HSP26

(A) At 25°C the mass spectrum of *Sc*HSP26 was dominated by signal arising from a broad range of oligomers with a minor percentage of monomer and dimer.

(B) At higher temperatures (43°C and 60°C), the relative amount of signal arising from the *Sc*HSP26 oligomers was greatly diminished with a concomitant increase in the percentage of monomer and dimer.
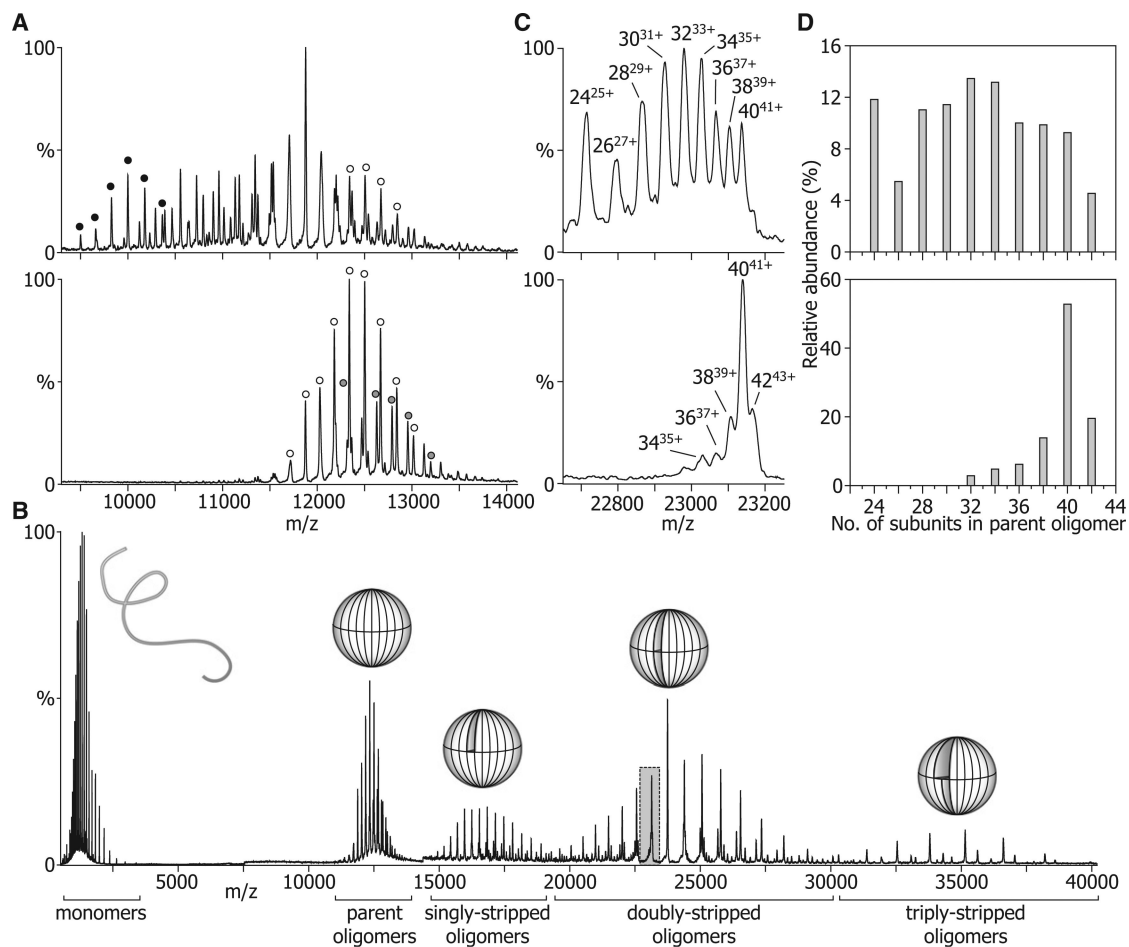
Figure 4. Defining the Oligomeric Distributions of *Sc*HSP26

(A) NanoESI-MS demonstrated that *Sc*HSP26 exists as a broad range of oligomers at 25°C (upper), but forms mainly 40 mers (open circles), and 42 mers (shaded circles) at 43°C (lower). Note that a 24-mer is notably abundant at room temperature (black circles).

(B) Collision-induced dissociation of monomers from the native oligomers gives rise to a series of stripped oligomers of reduced charge with sufficient peak resolution to accurately define their size distribution. Overlaid are schematic representations of the different species.

(C) Portion of the doubly-stripped region highlighted in (B) for *Sc*HSP26 at 25°C (upper) and 43°C (lower). From the peaks in this region of the spectra, it was possible to assign charge states to individual oligomers, as well as calculate their relative abundance.

(D) Histograms showing the most abundant oligomers present at 25°C and 43°C after analysis of the stripped oligomer region.
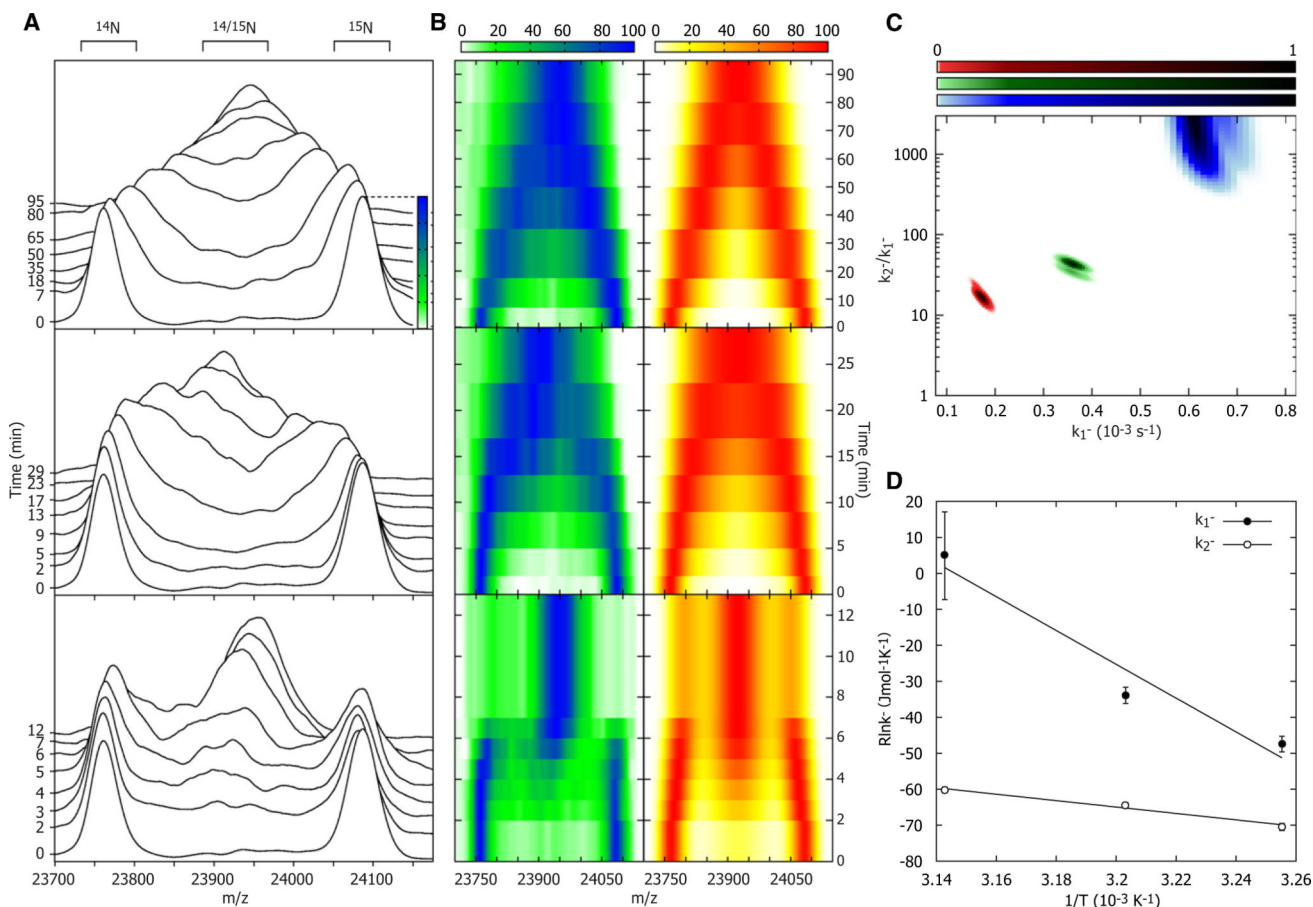
Figure 5. Subunit Exchange

(A) The overlapping peaks of the doubly stripped oligomers were monitored at 34°C (top), 39°C (middle), and 45°C (bottom) until exchange was complete. ^{14}N and ^{15}N-labeled ScHSP26 homo-oligomer peaks diminished with time, and in their place a peak corresponding to hetero-oligomers of the two subunits arose. This peak was broad because of the variety of isotopic stoichiometries in the polydisperse assembly. As expected, the rate of exchange was found to increase with temperature; notably, however, there appeared to be a change in the mechanism of exchange at 45°C. This was evidenced by the fact that in the period between 2 and 4 min a population of fully exchanged ScHSP26 coexisted with the original homo-oligomers.

(B) Alternative "top down" contour plot representation of the data in (A), left, compared with the simulated subunit exchange time-course that best fits each temperature, right.

(C) Reduced χ^2 surface for the fitting of subunit exchange data to two rate constants, k_1^- and k_2^-.

(D) Arrhenius plots for the temperature dependence of k_1^- and k_2^- allows the extraction of the activation energies of the two processes. Mean values and error estimates are obtained by fitting a two-dimensional Gaussian function of the form a*exp($-(x-x_0)^2/(2c_x^2)$)*exp($-(y-y_0)^2/(2c_y^2)$) to the χ^2 probability surface. The central position of the Gaussian function indicates the mean value of the fitting parameter (x_0, y_0), and the widths the uncertainties (c_x, c_y).